

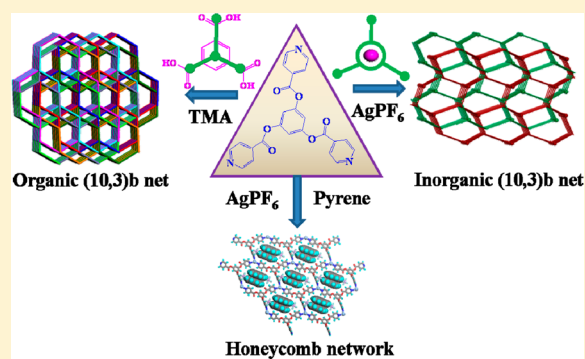
Topological Equivalences between Coordination Polymer and Co-crystal: A Tecton Approach in Crystal Engineering

Gargi Mukherjee and Kumar Biradha*

Department of Chemistry, Indian Institute of Technology, Kharagpur 721302, India

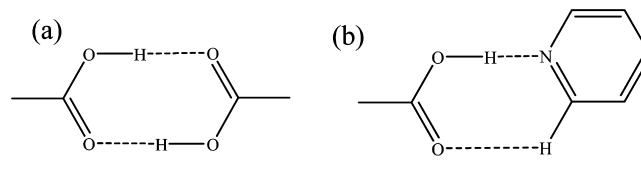
Supporting Information

ABSTRACT: The ligand benzene-1,3,5-triyltriisonicotinate (**1**) was shown to form topologically equivalent organic and metal–organic networks upon treatment with trimesic acid (H_3TMA) and $Ag(I)$ salt, respectively. Both exhibit interpenetrated (10,3)-b networks, signifying the tecton equivalency between $Ag(I)$ and H_3TMA . The metal–organic network is doubly interpenetrated, while the organic network is 8-fold interpenetrated which highlights the size differences between $Ag(I)$ and H_3TMA . Despite interpenetration, both the networks were found to incorporate solvents MeOH and $CHCl_3$ in their channels. Further, the repeat of reaction of $Ag(I)$ with **1** in the presence of a pyrene guest was found to produce crystals of open honeycomb (6,3) network with inclusion of pyrene molecules in the channels.



Prediction of the crystal structure for a given molecular structure is accepted to be one of the difficult tasks in the crystal engineering, as several factors govern the crystallization reaction outcome.¹ The failure of such predictions was provocatively referred to as “one of the continuing scandals” by Maddox in 1988.² The tecton approach that is purely based on molecular symmetry and the placement of functional groups on the molecule and the supramolecular synthon approach which deals with the robustness of the functional group interactions serve the purpose of structural prediction to some extent in cases of highly symmetrical molecules/supramolecular architectures.^{3–5} In short, in the tecton approach, molecular building blocks are highlighted, while in the synthon approach, interactions are given importance; however, the same underlying principle of molecular programming is there in both of them. Even in the case of symmetrical molecules, several other possible structures exist which differ significantly from predictable ones. For example, a 3-fold molecule can exhibit a honeycomb network as well as (10,3)-a or -b networks; similarly, a S_4 -symmetrical molecule can exhibit a diamondoid or 2D-layer structures.^{6,7} The generation of crystal structures of single organic components by using two or multi organic components, cocrystals or salts, is also one of the current challenges in crystal engineering. In this regard, the honeycomb network that was formed by trimesic acid (H_3TMA) via synthon-I was shown to be formed by H_3TMA (node) and 4,4'-bipy or other spacers using synthon-II (Scheme 1).^{8,9} Similarly, the formation of extended diamondoid networks via synthon-II using two components was also shown very recently.^{7,10} Further, the 3-fold symmetric molecules when linked (two-connected) through metal nodes were known to form (10,3)-a and (10,3)-b networks for a long while.¹¹ However, only recently the organic counterpart of (10,3)-a

Scheme 1. (a) Synthon I and (b) synthon II



network was reported, but to date no (10,3)-b network was reported to the best of our knowledge.¹²

On the other hand, the generation of topologically equivalent purely organic and metal–organic networks is also one of the challenging tasks of crystal engineering.¹³ Herein, we report one such example using the molecule, benzene-1,3,5-triyltriisonicotinate (**1**), which was linked to form topologically equivalent networks via 3-connected organic (H_3TMA) or inorganic nodes/tectons [$Ag(I)$]. In the case of H_3TMA and **1**, the networks are propagated through synthon-II, whereas in the case of $Ag(I)$ and **1**, the networks are propagated by coordination bonds. Recently, it was shown by us that the molecule **1** forms two-dimensional iso-structural CPs that exhibit remarkable ability of exchanging cations/anions in single-crystal-to-single-crystal manner and also exhibit breathing behavior in N_2 sorption.^{14,15} In continuation of our studies on CPs of **1**, the molecule **1** was reacted with $Ag(I)$ salts using the layering technique.

Layering of methanolic solution of $AgPF_6$ over the chloroform solution of **1** afforded needle-shaped crystals of

Received: December 13, 2013

Revised: January 9, 2014

Published: January 13, 2014

cocrystal **2**, $\{[\text{Ag}(\text{I})(\text{PF}_6)] \cdot (\text{CH}_3\text{OH}) \cdot (\text{H}_2\text{O}) \cdot (\text{CHCl}_3)\}_n$ (Figure 1). The single crystal X-ray analysis reveals that complex **2**

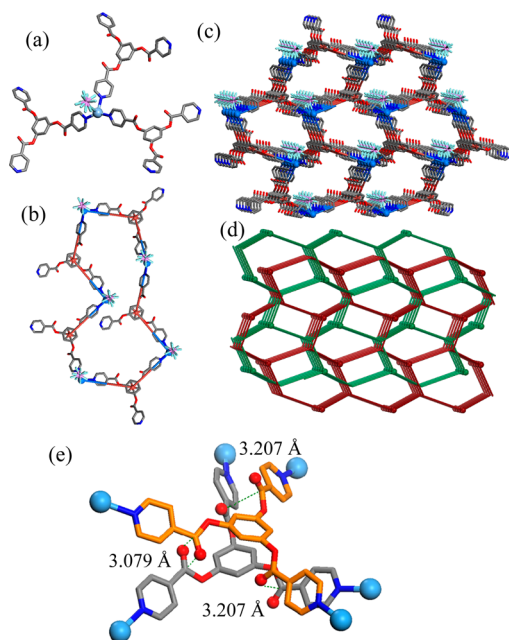


Figure 1. Illustrations for the crystal structure of **2**: (a) T-shape coordination geometry of Ag(I), (b) the shortest circuit formed by five each of Ag(I) atoms and molecules of **1**, (c) 3D-network with (10,3)-b topology, (d) 2-fold interpenetrated network, Ag(I) and **1** are represented as nodes, and (e) interpenetration of networks through $\pi \cdots \pi$ and dipole-dipole interactions between the central phenyl rings and the keto groups of ester, respectively.

is crystallized in the $C2/c$ space group. The asymmetric unit is constituted by one unit each of **1**, Ag(I), and PF_6 anion. The Ag(I) ion adopts a distorted trigonal pyramid geometry: the three pyridyl groups occupy the trigonal plane ($\text{N}-\text{Ag}$: 2.375, 2.210, and 2.209 Å; $\text{N}-\text{Ag}-\text{N}$: 99, 114, and 146°) and the disordered PF_6 anion is coordinated at the apical position. The Ag(I) ion is elevated from the N_3 plane by 0.128 Å, and the pyridyl rings make angles of 47°, 28°, and 36° with the N_3 plane. In the crystal structure, both Ag(I) and **1** act as 3-connected nodes and propagate the (10,3)-b framework. The shortest circuit is composed of five units each of Ag(I) and **1**. It is interesting to note here that within the (10,3)-b network, the coordinated PF_6 ions point in one-direction such that the chirality of the network is maintained. The remaining space of the cavities of network was filled by self-interpenetration of the network which has the opposite sense and solvent molecules which occupy 15.6% of the crystal volume. The interpenetration of the networks is assisted by the $\pi-\pi$ interactions between the central phenyl rings (3.979 Å) and dipole-dipole interactions between the $\text{C}=\text{O}$ groups of ester (3.079; 3.207 Å) (Figure 1e). It is interesting to note that the $\text{C}=\text{O}$ that exhibits shorter dipole-dipole interaction has longer $\text{C}-\text{O}$ distance (1.174 vs 1.257 Å), although the IR spectra shows only one peak at 1751 cm^{-1} .

As the Ag(I) serves as the 3-connected node in the structure, it was thought that H_3TMA as a probable tecton to produce organic cocrystal of **1** and H_3TMA containing (10,3)-b network via synthon-II. Crystals of cocrystal **3**, $\{[\text{1} \cdot \text{H}_3\text{TMA}] \cdot (\text{CH}_3\text{OH}) \cdot 2(\text{CHCl}_3)\}_n$ suitable for single crystal X-ray diffraction were obtained by dissolving 1:1 equivalents of **1** and H_3TMA in

$\text{CHCl}_3-\text{MeOH}$ (Figure 2). The crystal structure analysis of **3** reveals that it is crystallized in $P2_1/c$ space group, and it is a

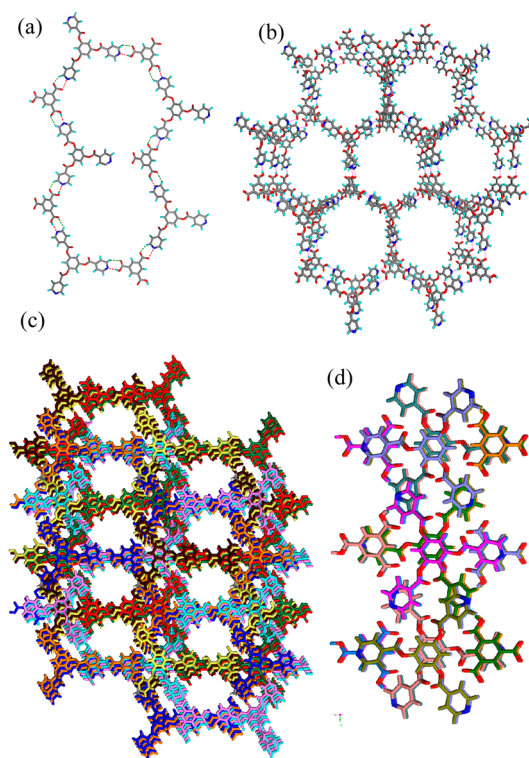


Figure 2. Illustrations for the crystal structure of **3**: (a) the shortest circuit formed by five molecules of **1** and five H_3TMA molecules, (b) organic network with (10,3)-b topology, (c) 8-fold interpenetrated network, and (d) interpenetration of networks through $\pi \cdots \pi$ interactions between the C_6 rings, between the pyridyl arms, and H_3TMA and pyridyl arms of **1**.

cocrystal. The $\text{C}-\text{O}$ and $\text{C}=\text{O}$ bond lengths of $-\text{COOH}$ of H_3TMA in **3** are 1.303 and 1.207; 1.304 and 1.216; and 1.304 and 1.214 Å, which clearly indicates that the $-\text{COOH}$ groups are not deprotonated. The molecules assemble through synthon-II (3.273, 2.6771; 2.694, 3.295; 3.226, 2.632 Å) to form a (10,3)-b network containing two organic components. The ligand geometry in the cocrystal deviates from the 3-fold symmetry similar to the one observed in complex **1**. The interplanar angles between the central phenyl plane and the pyridyl planes are 31.38°, 35.38°, and 39.45°. In **3**, the shortest circuit is composed of five each of H_3TMA and **1**. We note here that the both nodes in **3** show trigonal planar environment with angles close to 120°, whereas in **2**, Ag(I) severely deviates from trigonal planar geometry (150.15°, 113.25°, and 93.42°), although **1** has nearly 120° angles. In **3**, the (10,3)-b networks are 8-fold interpenetrated in contrast to 2-fold interpenetration of **1**. The increase in interpenetration could be the consequence of longer arm length of the H_3TMA tecton compared to the Ag(I) ion. The interpenetration occurs through the plethora of $\pi \cdots \pi$ interactions as follows: The units of **1** stack on each other in a staggered fashion such that central C_6 units interact with each other (3.837 Å). In between the pyridyl arms of the stacks, the adjacent pyridyl arms (3.768 Å) and H_3TMA interdigitate (3.754 Å) in a 4:2 ratio via $\pi \cdots \pi$ interactions (Figure 2e).

With the production of the topological equivalent (10,3)-b networks of **1** with 3-connected tectons, the possibility of eschewing the interpenetration of these networks in favor of

guest inclusion was explored by carrying these reactions in the presence of aromatic guest molecules.¹⁶ The layering of methanolic solution of AgPF₆ over the chloroform solution of **1** and pyrene afforded colorless, block-shaped crystals of complex **4**, {[Ag₂(**1**)₂]-2(PF₆)-3(pyrene)-2(CHCl₃)}_n. The single crystal X-ray analysis reveals that the complex **4** crystallized in *P* $\bar{1}$, and the asymmetric unit is constituted by one each of **1**, Ag(I) and the PF₆ anion, and 1.5 units of pyrene. In **4**, Ag(I) exhibits planar coordination geometry, unlike the trigonal pyramid geometry in **2**. However, similar to **2**, both Ag(I) ion and **1** act as a three-connected node but forms an open honeycomb network with an arm length of 9.8 Å (Figure 3). As anticipated, the interpenetration was eschewed in favor

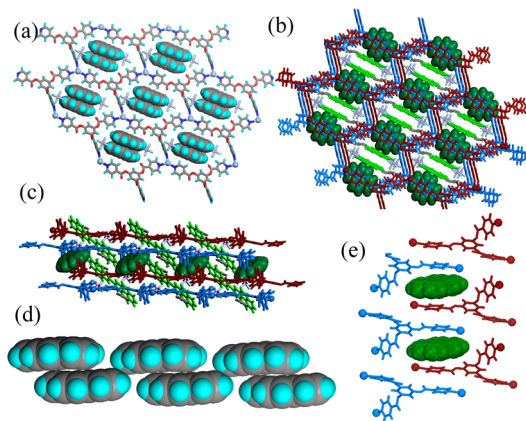


Figure 3. Illustrations for the crystal structure of **4**: (a) honeycomb network formed by Ag(I) and **1** with pyrene dimers inside the hexagonal cavities; packing of layers (b) top view and (c) side view, channeled pyrenes were shown in parrot green and cylinder mode, the pyrenes between the bilayers were shown in dark green and a space filling mode; (d) column of pyrene dimers; and (e) intercalation of pyrene between the bilayers via $\pi\cdots\pi$ and $C=O\cdots\pi$ interactions.

of the inclusion of the pyrene guest molecule. The honeycomb layers form double layers via $Ag\cdots\pi$ (4.507 Å) and $O=C\cdots\pi$ (3.460 Å) interactions. These double layers pack in slipped manner such that there exists continuous channels which are occupied by a column of pyrene dimers and PF₆ ions. Between the double layers, one of the pyrene molecules is sandwiched by $\pi\cdots\pi$ interactions between pyrene and Py-CO- moieties of **1** (4.659 Å). We note here that recently reported structures of **1** with Ag(I) salts have honeycomb networks which have offset packing unlike the ones reported here. In those examples, solvent molecules were found to act as guest molecules and form unstable crystals.¹⁷

Efforts to obtain cocrystal of H₃TMA with **1** in the presence of pyrene or other aromatic guest molecules were not successful. We note here that complex **4** bears striking structural resemblance with that of [TMA·tpt]·2pyrene, as both are honeycomb networks, and the channels are occupied by pyrene molecules.¹⁸ However, the differences between the present structure and that of [TMA·tpt]·2pyrene is that in [TMA·tpt]·2pyrene the channels are filled by four molecules of pyrene. In contrast in the present structure, those are filled by two pyrene and two PF₆ anions. Longer length of H₃TMA and the absence of anions may be reason of inclusion of two extra pyrene molecules in that structure.

Solid state diffuse reflectance spectra (DRS) of **2** and **3** were recorded at room temperature and compared with those of

H₃TMA and **1** (Figure 4). The bands of **2** and **3** varied considerably from those of **1** and H₃TMA. **1** and H₃TMA

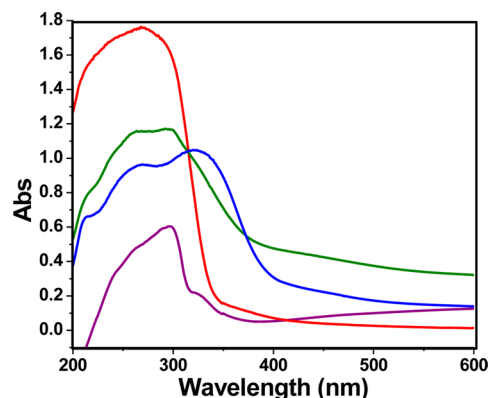


Figure 4. Diffuse reflectance spectra of **1** (red line), H₃TMA (purple line), **2** (blue line), and **3** (green line).

showed peaks at 268 and 298 nm, respectively. However, both **2** and **3** were found to exhibit three absorption peaks; for **2** the absorption peaks were observed at 211, 256, and 330 nm, while those of **3** are located at 213, 260, and 294 nm.

In conclusion, it was demonstrated that H₃TMA is an equivalent tecton to Ag(I) to produce topologically equivalent (10,3)-b networks upon self-assembling with **1**. The size of the tecton altered the degree of interpenetration, smaller Ag(I) produced doubly interpenetrated and the bigger tecton H₃TMA produced an 8-fold interpenetrated network. The ligand–ligand interactions and Ag(I)–ligand interactions played a significant role in the interpenetration of networks. The cocrystal **3** is the first of its kind as there is no report on cocrystal of **1** to date, and also it represents the first example of the organic two component (10,3)-b network. The presence of the guest such as pyrene was found to influence the network geometry and interpenetration in the case of Ag(I) and **1** but not in case of H₃TMA and **1**. Smaller aromatic guests than pyrene failed to produce single crystals, even in case of the reaction of Ag(I) and **1**.

■ ASSOCIATED CONTENT

📄 Supporting Information

Experimental details, IR spectra, XRPD patterns, and TGA data. This material is available free of charge via the Internet at <http://pubs.acs.org>.

■ AUTHOR INFORMATION

Corresponding Author

*E-mail: kbiradha@chem.iitkgp.ernet.in. Fax: +91-3222-282252. Tel: +91-3222-283346.

Notes

The authors declare no competing financial interest.

■ ACKNOWLEDGMENTS

We gratefully acknowledge the DST for the financial support and DST-FIST for the single-crystal X-ray facility. G.M. thanks CSIR for a research fellowship.

■ REFERENCES

- (1) Jones, P. L.; Byrom, K. J.; Jeffery, J. C.; McCleverty, J. A.; Ward, M. D. *Chem. Commun.* **1997**, 1361–1362. (b) Beer, P. D.;

- Hayes, E. J. *Coord. Chem. Rev.* **2003**, *240*, 167–189. (c) Díaz, P.; Benet-Buchholz, J.; Vilar, R.; White, A. J. P. *Inorg. Chem.* **2006**, *45*, 1617–1626. (d) Lopez, S.; Keller, S. W. *Inorg. Chem.* **1999**, *38*, 1883–1888. (e) Dalgarno, S. J.; Hardie, M. J.; Raston, C. L. *Cryst. Growth Des.* **2004**, *4*, 227–234. (f) Mahata, P.; Sundaresan, A.; Natarajan, S. *Chem. Commun.* **2007**, 4471–4473.
- (2) Maddox, J. *Nature* **1988**, 335, 201.
- (3) Simard, M.; Su, D.; Wuest, J. D. *J. Am. Chem. Soc.* **1991**, *113*, 4696–4698.
- (4) Wuest, J. D. *Chem. Commun.* **2005**, 5830–5837.
- (5) Desiraju, G. R. *Angew. Chem., Int. Ed.* **1995**, *34*, 2311–2327.
- (6) Rao, K. P.; Higuchi, M.; Duan, J.; Kitagawa, S. *Cryst. Growth Des.* **2013**, *13*, 981–985.
- (7) (a) Roy, S.; Biradha, K. *Cryst. Growth Des.* **2013**, *13*, 3232–3241. (b) Reddy, D. S.; Dewa, T.; Endo, K.; Aoyama, Y. *Angew. Chem., Int. Ed.* **2000**, *39*, 4266–4268.
- (8) (a) Duchamp, D. J.; Marsh, R. E. *Acta Crystallogr., Sect. B* **1969**, *25*, 5–19. (b) Herbstein, F. H. *Top. Curr. Chem.* **1987**, *140*, 107–139.
- (9) (a) Weyna, D.; Shattock, R. T.; Vishweshwar, P.; Zaworotko, M. J. *Cryst. Growth Des.* **2009**, *9*, 1106–1123. (b) Sharma, C. V. K.; Zaworotko, M. J. *Chem. Commun.* **1996**, 2655–2656. (c) Santra, R.; Ghosh, N.; Biradha, K. *New J. Chem.* **2008**, *32*, 1673–1676.
- (10) (a) Roy, S.; Mahata, G.; Biradha, K. *Cryst. Growth Des.* **2009**, *9*, 5006–5008. (b) Men, Y.-B.; Sun, J.; Huang, Z.-T.; Zheng, Q.-Y. *CrystEngComm* **2009**, *11*, 978–979.
- (11) (a) Carlucci, L.; Ciani, G.; Proserpio, D. M.; Sironi, A. *J. Am. Chem. Soc.* **1995**, *117*, 12861–12862. (b) Carlucci, L.; Ciani, G.; Proserpio, D. M.; Sironi, A. *J. Am. Chem. Soc.* **1995**, *117*, 4562–4569. (c) Abrahams, B. F.; Batten, S. R.; Hamit, H.; Hoskins, B. F.; Robson, R. *Chem. Commun.* **1996**, 1313–1314. (d) Yaghi, O. M.; Li, H. *J. Am. Chem. Soc.* **1996**, *118*, 295–296. (e) Yaghi, O. M.; Davis, C. E.; Li, G.; Li, H. *J. Am. Chem. Soc.* **1996**, *119*, 2861–2868. (f) Abrahams, B. F.; Jackson, P. A.; Robson, R. *Angew. Chem., Int. Ed.* **1998**, *37*, 2656–2659. (g) Biradha, K.; Fujita, M. *Angew. Chem., Int. Ed.* **2002**, *41*, 3392–3395. (h) Abrahams, B. F.; Haywood, M. G.; Hudson, T. A.; Robson, R. *Angew. Chem., Int. Ed.* **2004**, *43*, 6157–6160. (i) Eubank, J. F.; Walsh, R. D.; Eddaoudi, M. *Chem. Commun.* **2005**, 2095–2097. (j) Ke, Y.-X.; Collins, D.-J.; Sun, D.-F.; Zhou, H.-C. *Inorg. Chem.* **2006**, *45*, 1897–1899. (k) Halper, S. R.; Do, L.; Stork, J. R.; Cohen, S. M. *J. Am. Chem. Soc.* **2006**, *128*, 15255–15268.
- (12) Shattock, T. R.; Vishweshwar, P.; Wang, Z.; Zaworotko, M. J. *Cryst. Growth Des.* **2005**, *5*, 2046–2049.
- (13) (a) Reddy, D. S.; Craig, D. C.; Rae, A. D.; Desiraju, G. R. *J. Chem. Soc., Chem. Commun.* **1993**, 1737–1739. (b) Reddy, D. S.; Craig, D. C.; Desiraju, G. R. *J. Chem. Soc., Chem. Commun.* **1995**, 339–340.
- (14) Mukherjee, G.; Biradha, K. *Chem. Commun.* **2012**, *48*, 4293–4295.
- (15) Mukherjee, G.; Biradha, K. *Chem. Commun.* **2014**, *50*, 670–672.
- (16) Santra, R.; Biradha, K. *Cryst. Growth Des.* **2009**, *9*, 4969–4978.
- (17) Xiong, Y.; Yang, R.; Chen, S.; Jiang, J.; Su, C. -Y. *CrystEngComm* **2013**, *15*, 9751–9756.
- (18) Ma, B.-Q.; Coppens, P. *Chem. Commun.* **2003**, 2290–2291.